BIOCHEMISTRY
including biophysical chemistry & molecular biology

Article

pubs.acs.org/biochemistry

Structure-Based Energetics of mRNA Decoding on the Ribosome

Priyadarshi Satpati, Johan Sund, and Johan Åqvist*

Department of Cell and Molecular Biology, Uppsala University, Biomedical Center, Box 596, SE-751 24 Uppsala, Sweden

Supporting Information

ABSTRACT: The origin of high fidelity in bacterial protein synthesis on the ribosome remains a fundamental unsolved problem despite available three-dimensional structures of different stages of the translation process. However, these structures open up the possibility of directly computing the energetics of tRNA selection that is required for an authentic understanding of fidelity in decoding. Here, we report extensive computer simulations that allow us to quantitatively calculate tRNA discrimination and uncover the energetics underlying accuracy in code translation. We show that the tRNA−mRNA interaction energetics varies drastically along the path from initial selection to peptide bond formation. While the selection process is obviously controlled by kinetics, the underlying thermodynamics explains the origin of the high degree of accuracy. The existence of both low- and high-selectivity states provides an efficient mechanism for initial selection and proofreading that does not require codon-dependent long-range structural signaling within the ribosome. It is instead the distinctly unequal population of the high-selectivity states for cognate and noncognate substrates that is the key discriminatory factor. The simulations reveal the essential roles played both by the 30S subunit conformational switch and by the common tRNA modification at position 37 in amplifying the accuracy.

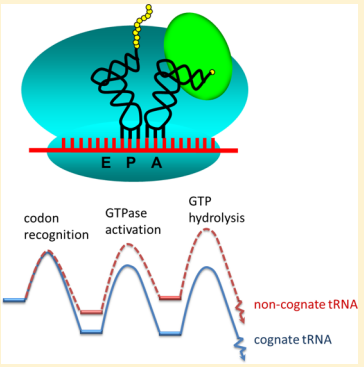

Translation of the genetic code on the ribosome is a highly accurate process that depends on selection of correct tRNAs to match the codon triplets of the mRNA presented at the decoding center. This selection occurs in two steps, initial selection and proofreading, that are separated by the irreversible hydrolysis of GTP.[1] In the first step, aminoacyl-tRNAs are delivered to the bacterial ribosome in a ternary complex with elongation factor Tu (EF-Tu) and GTP. After codon−anticodon contacts have formed at the decoding site for cognate complexes, EF-Tu very rapidly becomes activated for GTP hydrolysis. Noncognate tRNAs that have not been rejected at this stage are subjected to proofreading after GTP hydrolysis. In this step, they again have a much higher probability than cognate tRNAs of dissociating from the ribosome, instead of proceeding to peptide bond formation. tRNAs that are not rejected at either of these steps will attach the nascent peptide chain to their amino acid, and hence, the frequency of incorporation of erroneous amino acids directly reflects the combined accuracy of the two selection steps.

The high speed and high degree of accuracy of protein synthesis are critical for the living cell, and the evolutionary optimization of these variables has a direct bearing on the fitness of rapidly growing species, such as bacteria.[2] It has become clear from experimental studies that there is a trade-off between speed and accuracy leading to a typical peptide elongation rate of ∼20 s^{-1} with an average error frequency of roughly 10^{-4}.[2−5] These parameters also vary depending both on the amino acid that is incorporated in the elongation step and, in the case of misreading, on the nature of the noncognate tRNA−mRNA mismatch.[4−6] It was early realized that the intrinsic energetics of base pairing in an aqueous solution could not account for the low error frequency observed in protein synthesis on the ribosome. The explanation for the unexpectedly high degree of accuracy instead appears to be achieved by a combination of (i) amplified binding affinity differences between cognate and noncognate tRNAs on the ribosome,[7−9] (ii) discrimination in terms of the modulation of forward rate constants for GTP hydrolysis and peptidyl transfer relative to aminoacyl-tRNA rejection rates,[10,11] and (iii) the use of kinetic proofreading, in which GTP hydrolysis by EF-Tu provides the required irreversible chemical step that allows binding affinity differences to be exploited twice.[12,13] At present, we are, however, still far from a detailed structure-based description of the energy landscape underlying the peptide elongation process on the ribosome.

The advances in structural investigations of bacterial ribosomes during the past decade include the elucidation of a number of key complexes and conformational states involved in protein synthesis. As far as decoding is concerned, medium-resolution (∼3 Å) crystal structures of the free 30S subunit[14] and its complexes with tRNA anticodon stem loops,[7] the 70S ribosome with a bound EF-Tu·GTP·aa-tRNA ternary complex (using the GTP analogue GDPCP),[15] and 70S complexes with both cognate and noncognate A-site tRNAs accommodated in the peptidyl transferase center[16−18] essentially delineate the pathway from initial selection to proofreading and peptidyl transfer. Several of the key states involved have also been trapped in cryo-EM structures and seen in single-molecule Förster resonance energy transfer (FRET) experiments.[19−22] The near-

Received: January 9, 2014
Revised: February 20, 2014
Published: February 24, 2014

   dx.doi.org/10.1021/bi5000355 | *Biochemistry* 2014, 53, 1714−1722

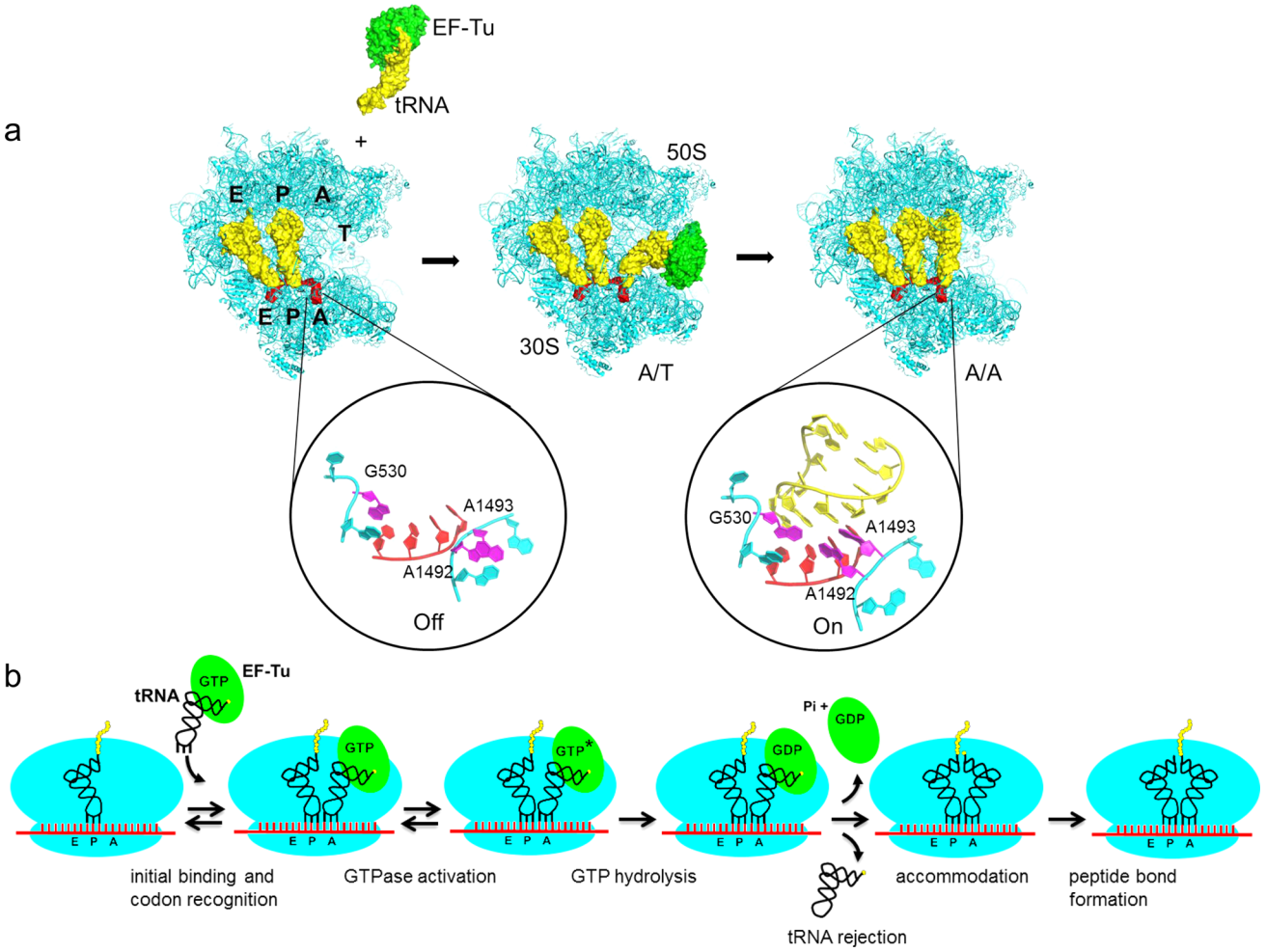

Figure 1. Different states along the peptide elongation path. (a) Delivery of tRNA in a ternary complex with EF-Tu and GTP (leading to the A/T conformation) and its subsequent accommodation into the ribosomal A-site (leading to the A/A conformation) are indicated. The insets show the structural changes of rRNA bases A1492, A1493, and G530 from crystallographic work,[7] which define the ribosomal On and Off states. (b) Reaction scheme depicting the main steps from tRNA binding to peptide bond formation, based on experimental studies.[3,10]

atomic resolution crystallographic complexes now provide sufficiently good models for structure-based computational evaluation of the energetics associated with the states in which they are trapped, and here we report computer simulations based on these crystal structures to decipher the energetics of decoding, thereby providing the key missing links between three-dimensional structures and experimentally measured kinetics.

MATERIALS AND METHODS

Free Energy Calculations. Relative binding free energies of mRNA mutations in the ribosome−tRNA complexes were calculated with the free energy perturbation method as described previously[23] using the MD simulation software Q.[24] U to C mutations were introduced at all three mRNA codon positions (UUU → CUU, UUU → UCU, and UUU → UUC) for the $tRNA^{Phe}$ complex in the A/T:Off, A/T:On, A/A:Off, and A/A:On states (Figures 1 and 2). Corresponding simulations were also conducted for the mRNA-programmed ribosome with an empty A-site to be able to calculate $\Delta\Delta G_{bind}$ through the appropriate thermodynamic cycle.[23] To investigate the effect of the tRNA modification at position 37, we repeated calculations with ms^2i^6A37 changed to an unmodified adenine base.

Initial coordinates for simulations of the A/A:On state were retrieved from the crystal structure of the accommodated $tRNA^{Phe}$ complex of Protein Data Bank (PDB) entry 3I8H.[17] The A/A:Off state was modeled using the same coordinates, but substituting G530, A1492, and A1493 with those from the superimposed structure of the free 30S subunit (PDB entry 1FJF).[14] There are several crystal structures with an empty A-site[14,25,26] (PDB entry 1FJF has the highest resolution of these) that show the monitoring bases in somewhat different Off positions, indicating that this state may be conformationally variable, but the On-state positions of these bases are very well-defined.[7,17,18,26] $tRNA^{Phe}$ in the A/T state was modeled using the $tRNA^{Trp}$ complex (in the A/T state) with PDB entry 2XQD[15] as a template, substituting the last five nucleotides of the mRNA and nucleotides 32−37 of the $tRNA^{Trp}$ anticodon loop. Ion positions for the A/T state were taken from PDB entry 3I8H as the structure of PDB entry 2XQD lacks ions. The A/T:Off state was modeled as described above for the A/A:Off state but using the structures of PDB entries 2XQD and 1FJF.

Relative binding free energies for $tRNA^{Phe}$ with cognate and near-cognate A-site codons were also calculated for possible mixed On−Off structures in which either A1493 or G530 was in the On conformation (Figure S1 of the Supporting Information). To verify that codon mutations in the A-site are insensitive to the ribosome On−Off transition in the absence of tRNA, simulations with empty A-sites were conducted for the On and Off

dx.doi.org/10.1021/bi5000355 | Biochemistry 2014, 53, 1714−1722

conformations of the ribosome, and the mutation free energies are summarized in Table S3 of the Supporting Information. The antibiotic paromomycin was removed from the structures in all calculations. The effect of possible protonation of near-cognate A-C mismatches was examined by calculations in which the second anticodon position in $tRNA^{Phe}$ was protonated in the ribosome complex (A-C → A^+-C) and free in water (A → A^+). The stability of the protonated A^+-C base pair can then be determined from the relevant thermodynamic cycle using the pK_a of 3.5 for N1 of adenosine in water as described below.

Molecular Dynamics (MD) Simulations. All MD simulations were performed on spherical simulation systems as implemented in Q.[24] Spheres with radii of 25 Å centered on the N1 atom of the first codon position were cut from the crystal structures and solvated by a 37 Å radius water droplet, where water molecules to the sphere boundary were subjected to radial and polarization restraints according to the SCAAS model.[24,27] Solute atoms between 22 and 25 Å from the center were tightly restrained throughout the simulations, leaving the inner 22 Å radius shell including A- and P-site atoms fully flexible. Extra Mg^{2+} ions positioned 25−35 Å from the sphere center were also taken from the crystal structure of PDB entry 3I8H[17] to obtain a simulation sphere with zero net charge. These ions were allowed to move freely in the simulations. The positions of internal ions turn out to be rather stable, with no major shifts observed. Phosphate groups more than 22 Å from the simulation center were neutralized by scaling down the partial charges. MD simulations were performed with a 1 fs time step and a direct cutoff of 10 Å for nonbonded interactions, with long-range electrostatic interactions beyond this cutoff treated by the local reaction field multipole expansion method.[28] No cutoff was applied to the base that was mutated. For both free and tRNA-bound systems, each free energy calculation (with 51 discrete windows) was based on 10−30 ns of data collection comprising 8−24 replicates with different initial conditions. The standard errors of the mean calculated from these replicate simulations are generally less than ±1 kcal/mol (cf. Figure 2). Further indications of good convergence are that forward and reverse free summation for individual replicate always differs by <1 kcal/mol and that if the data for each replicate are divided into two equal batches (corresponding to the first and second halves of the data collection trajectories) the free energy deviations between these are also <1 kcal/mol.

The calculations used the CHARMM22 force field,[29,30] and additional simulations were also carried for $tRNA^{Phe}$ in the A/A:On state with the AMBER99_SB_BSC0 force field[31,32] to examine force field dependence (Table S2 of the Supporting Information).The robustness of the $tRNA^{Phe}$ simulations in the A/A:On state was further examined by repeating the calculations using the crystal structure of PDB entry 2WDG[16] as a starting point and a smaller simulation sphere (20 Å radius), with 25 ns data collection for each transformation (Table S1 of the Supporting Information). The system was in this case neutralized differently by selecting Mg^{2+} ions from the crystal structures of PDB entries 2WDG,[16] 1IBM,[33] 2J00,[34] and 3I8G;[17] A37 was modified to ms^2i^6A, and the incomplete protein S13 was removed. This simulation scheme was also used for the calculations with a protonated A-C base pair. Here, the two simulation systems with the GAA anticodon (ribosome complex and free tRNA) were both overall neutral and had the same radius. This is essential for long-range electrostatic contributions (from outside the simulation sphere) to the solvation energy change associated with transformation to the GA^+A anticodon to cancel.[35]

RESULTS

Structural and Kinetic Views of Decoding. Available experimental data suggest two structural features of the ribosome complexes with A-site tRNA to be particularly relevant for the energetics of discrimination between correct and incorrect tRNAs. These are (Figure 1), first, the conformational change that a tRNA molecule undergoes upon accommodation into the peptidyl transferase center on the 50S subunit after GTP hydrolysis and release of EF-Tu and, second, the "switching on" of the so-called monitoring rRNA bases of the 30S subunit concomitant with a small 30S interdomain movement.[7] These monitoring bases, A1492, A1493, and G530, adopt significantly different conformations in the case of an empty A-site (Off state)[14,25,26] and an A-site into which a tRNA (or anticodon stemloop) has relaxed after release of EF-Tu (On state).[7,16−18] The conformational change of these bases presumably contributes to the enhancement of the discriminatory power of the mRNA-programmed ribosome,[7,9] although the effect has never actually been quantified. Moreover, the monitoring bases can be forced into the On state by binding of the error-inducing antibiotic paromomycin, which effectively displaces A1492 and A1493 from their Off-state position in helix 44.[7,36]

The kinetic picture of peptide chain elongation on the ribosome that has emerged from a number of experimental studies[3,5,6,8,10,11] is more complex than that indicated by the structures in Figure 1a. Rodnina and co-workers have identified up to seven steps on the pathway from initial binding of the ternary complex to peptidyl transfer,[3,10] and the main steps limiting the rate of peptide formation can be condensed into the reaction scheme shown in Figure 1b. Here, initial binding and codon recognition bring the system to its first selection point, where off-rates between cognate and near-cognate ternary complexes differ by a factor of up to 1000 (corresponding to a difference in binding free energy of ∼4 kcal/mol, because on-rates are equal).[8,10] After the GTPase activation and irreversible GTP hydrolysis steps, which limit the rate for noncognate complexes but not for cognate complexes,[8,10] the aa-tRNA can either go on to form the peptide bond or be rejected with unequal probabilities for correct and incorrect substrates (proofreading). Apart from the fact that the ternary complex docks to the ribosome with the tRNA in the bent (A/T) conformation upon codon recognition[15,19] (Figure 1a) and that eventually peptide bond formation requires relaxation of cognate aa-tRNA into the accommodated straight (A/A) conformation, it is not known at which stage ribosome monitoring is turned on or from which conformational states incorrect tRNAs are rejected.

Structure-Based Energetics of Decoding. To attack the problem of decoding energetics and elucidate the roles of different conformational states in the selection process, we conducted extensive molecular dynamics (MD) free energy simulations of cognate and near-cognate ribosome complexes using different crystallographic structures[7,14−17] as starting points. These calculations involve computing the change in binding affinity for $tRNA^{Phe}$ (GAA anticodon) in the ribosomal A-site upon U/C mutations in all three codon positions. The simulations were performed for different possible combinations of the A/T and A/A states with the ribosome in On and Off conformations. Further, the effect of the critical tRNA modification at position 37 (2-methylthio-N6-isopentenyladenosine, ms^2i^6A, in most bacteria) was examined in all cases.

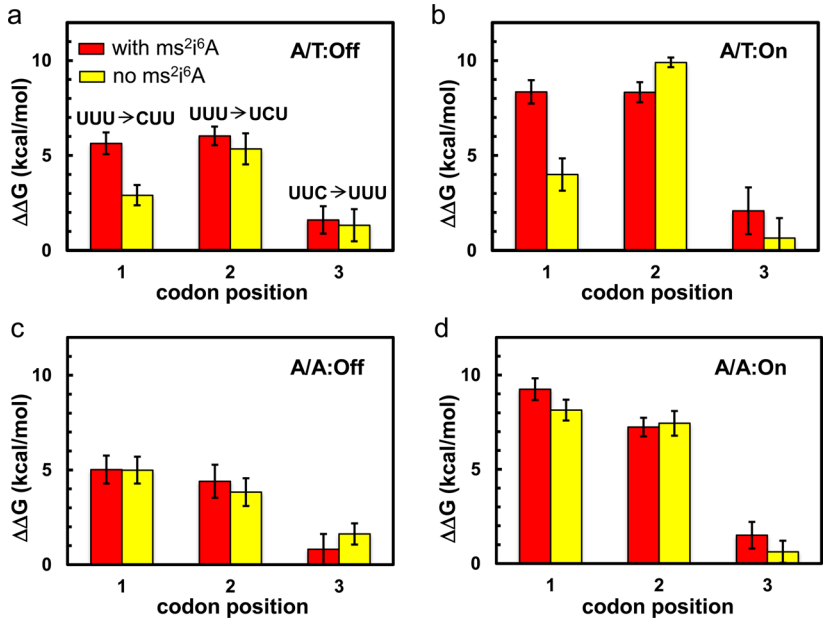

Figure 2. Calculated energetics of codon reading in different states. Panels a–d show the calculated $tRNA^{Phe}$ binding free energy differences for U to C mutations in all three mRNA codon positions in the A/T:Off, A/T:On, A/A:Off, and A/A:On states, respectively. The cognate codons are UUU and UUC. Red and yellow bars denote, respectively, simulations with and without the tRNA modification in position 37. Error bars show one standard error of the mean.

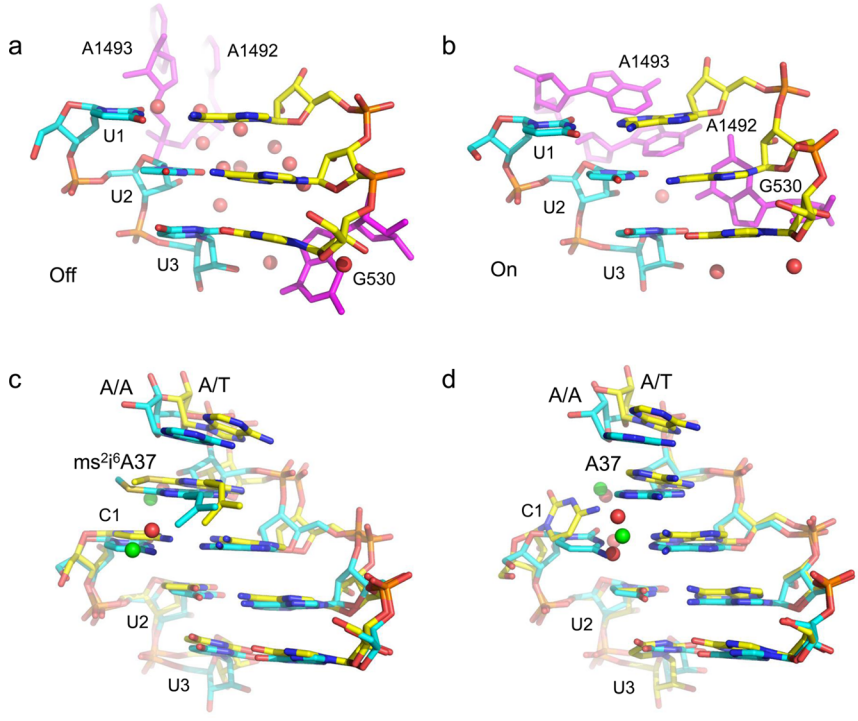

Figure 3. Structural mechanisms for selectivity amplification. Average molecular dynamics structures showing how the A4192, A1493, and G530 rRNA bases (magenta) effectively exclude solvent molecules from interacting with the minor groove of the codon–anticodon helix when going from the Off state (a) to the On state (b). The codon (UUU) and anticodon (GAA) are shown with cyan and yellow carbons, respectively, and water molecules as red spheres. (c and d) Average structures showing an A-C mismatch at position 1 for the A/T (yellow carbons, water as red spheres) and A/A (cyan carbons, water as green spheres) On states, with (c) and without (d) the ms^2i^6A37 tRNA modification.

The results reveal several remarkable features (Figure 2). First, the effect of ribosome switching from the Off to the On state can be seen to drastically boost the discrimination in the first two codon positions. That is, with the monitoring bases turned off, the first two codon positions show a selectivity for the cognate codon of ~5 kcal/mol, for both the A/T and A/A tRNA conformations (Figure 2a,c). When the bases are switched on, this selectivity rises to around 8 kcal/mol (Figure 2b,d). Second, the tRNA modification at position 37 is found to have markedly different effects on the A/T versus the A/A conformation. It is

dx.doi.org/10.1021/bi5000355 | *Biochemistry* 2014, 53, 1714–1722

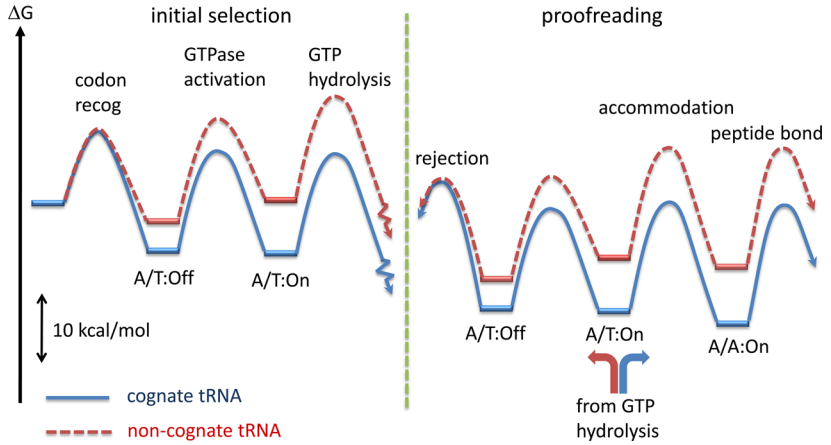

Figure 4. Energetics of translational accuracy. Schematic free energy diagram for initial selection (left) and proofreading (right) illustrating how the existence of both low-selectivity (Off) and high-selectivity (On) states can be used to drive dissociation of incorrect substrates. Average binding free energy differences between cognate and noncognate substrates of approximately 5 and 8 kcal/mol are assigned to the Off and On states, respectively, and the On states are downhill for cognate and uphill for noncognate substrates (see the text). Activation barriers for the elementary steps are depicted as ~15 kcal/mol[8,10] and are assumed to be the same for both substrates. The preferred direction for substrate flow after GTP hydrolysis is indicated at the proofreading stage (the possible additional rejection path involving the A/A:Off state is omitted for the sake of clarity because it does not change the energetic picture).

thus seen to mainly act by increasing the first position discrimination between tRNAs in the A/T conformation, which would otherwise be significantly lower than that of the second codon position (Figure 2a,b). Third, the wobble position has a uniformly low level of discrimination of around 1 kcal/mol, as expected from the ability of $tRNA^{Phe}$ to read both UUU and UUC codons, and this is essentially unaffected by the A/T to A/A and Off to On transitions, as well as the tRNA modification.

The MD simulations further reveal that the pronounced effect of switching on the three monitoring bases, in the bent (A/T) and straight (A/A) tRNA conformations, is due to a complete exclusion of solvent on the minor groove side of the first two base pairs (Figure 3a,b). This causes the penalty of mismatches to increase significantly because no water molecules can enter to compensate for missing hydrogen bond interactions in non-cognate base pairs. Hence, the term "monitoring bases" for A1492, A1493, and G530 actually appears to be somewhat misleading because their main energetic role is to shield the codon−anticodon interaction from solvent, thereby amplifying the discriminatory power, rather than to monitor correct Watson−Crick pairing. This is also in line with recent crystal structures that have trapped accommodated near-cognate tRNAs and show the bases in the On state even for near-cognate base pairs.[18] We find no major distortions of the anticodon loop in this state, and the discriminatory power is rather seen to arise from a lack of hydrogen bonding and repulsion as anticipated previously.[18]

As mentioned, the first codon position needs the ms^2i^6A modification at position 37 in the A/T states to achieve a selectivity on par with that of the second position (Figure 2). The structural origin of this effect (Figure 3c,d) is that the tRNA modification, situated "on top" of the first base pair, locks the A-C mismatch in its planar conformation with one hydrogen bond. Without the modification, the first mRNA base may relax away from its tRNA partner (A36), thereby allowing for formation of compensating hydrogen bonds with solvent molecules, even with the minor groove side shielded in the A/T:On state (Figure 3). In the accommodated A/A states, the first base pair becomes rigidified because of the straight tRNA structure (Figure 3c,d), which stabilizes the conformation of the codon−anticodon minihelix and renders the first and second position selectivities virtually equal. Hence, we can conclude that a key role of the ms^2i^6A modification is to remedy the suboptimal first position discrimination during initial selection. The second codon position, in contrast, has a higher intrinsic selectivity due to the fact that mismatches will be sequestered in their planar conformation between the flanking bases, even in the A/T states.

Connection between Calculated Energetics and Experimental Kinetics. A key question is now how the calculated structure-based energetics of Figure 2 can be unified with available experimental kinetic data. We first note that the calculated first and second position selectivities for the A/T:Off state of ~5 kcal/mol are in nearly quantitative agreement with ternary complex binding measurements of Rodnina and co-workers,[8] although the experiments utilized the His84Ala EF-Tu mutant and a yeast $tRNA^{Phe}$ with a different modified base at position 37. It may be noted that Ehrenberg and co-workers also found that first and second position discriminations (d values) were very similar to each other for near-cognate G-U mismatches.[5] The A/T:On state, on the other hand, has predicted selectivities of >8 kcal/mol for the first two positions with the tRNA modification, which is significantly larger than the experimental values. This thus strongly suggests that the codon recognition step in the scheme of Figure 1b corresponds to a binding process that ends up in the A/T:Off state. Moreover, the experimentally determined free energy barrier for GTPase activation and GTP hydrolysis (derived in ref 8 from k_3) was found to increase by 3−4 kcal/mol for first and second position A-C mismatches.[8] This increase in activation free energy agrees remarkably well with the predicted difference in discrimination between the A/T:On and A/T:Off states (Figure 2). This can be interpreted such that GTPase activation brings the system to the A/T:On state, with unequal probabilities for cognate and noncognate substrates, from which GTP hydrolysis eventually occurs with the same rate constant for the elementary chemical step (Figure 4). This would thus imply that the low measured value (<1 s^{-1}) of the GTP hydrolysis rate (k_3) for the noncognate codons[8] includes the probability factor $e^{-\Delta G/RT}$ of reaching the GTPase-activated (A/T:On) state (where ΔG = 3−4 kcal/mol). Another component of GTPase activation is a relatively small

dx.doi.org/10.1021/bi5000355 | *Biochemistry* 2014, 53, 1714−1722

Table 1. Numerical Example of the Accuracy for tRNA^{Phe} in Initial Selection[a]

rate constant (s^{-1})	cognate (UUC)	noncognate (CUC)	$\Delta G_{cognate}$ (kcal/mol)	$\Delta G_{noncognate}$ (kcal/mol)	
k_1 (codon reading, μM^{-1} s^{-1})	140	140	18.9	18.9	$\ddagger_1$
k_{-1}	0.12	100	0	4.0	A/T:Off
k_2 (GTPase activation)	120	120	14.8	18.8	$\ddagger_2$
k_{-2}	20	15000	−1.1	6.9	A/T:On
k_3 (GTP hydrolysis)	120	120	13.7	21.7	$\ddagger_3$
k_{cat}	55	0.9			
k_{cat}/K_M (μM^{-1} s^{-1})	140	1.3			

[a]Experimental rate constants for initial selection[8] correspond to the bimolecular association rate (k_1), the rate of dissociation from the codon recognition complex (k_{-1}), and the cognate rates for GTPase activation and GTP hydrolysis (k_2 and k_3, respectively). Columns 5 and 6 give the free energies of activation barriers (numbered 1−3 from the left in Figure 4) and intermediate states relative to the cognate A/T:Off state, respectively. Note that the noncognate GTPase activation barrier can be increased somewhat without any significant effect on the results.

rigid body-like movement of the GTPase domain of EF-Tu and the transition of His84 from its inactive to active catalytic conformation,[15,37] where the latter process has been shown to occur rapidly.[38]

The high level of discrimination in both the A/T:On and A/A:On states is a robust feature of these calculations. It is practically insensitive to the initial structural model, the presence of the S13 protein tail, which lies differently between the A- and P-site tRNAs in different crystal structures,[16,17] the size of the simulation system, the choice of crystallographic Mg^{2+} ion positions, and the force field used in the MD simulations (Tables S1 and S2 of the Supporting Information). Moreover, there are no low-energy tautomers of A-C base pairs that could alleviate the high selectivity,[39] but adenine protonation at N1 is a possibility that has to be considered.[40] As a check, we therefore also calculated the effect of mutating the second position anticodon A to A^+ (with protonation at N1) in the A/A:On state and for free tRNA^{Phe} in solution. This yielded an apparent stabilization of the A^+-C base pair of −4.2 ± 0.6 kcal/mol that, however, has to be corrected with the free energy cost of protonating the adenine in solution at pH 7. With a pK_a of 3.5 for N1, this correction thus becomes 4.8 kcal/mol, resulting in a net effect on the free energy of binding to the ribosome of 0.6 kcal/mol for the protonated base pair compared to the neutral one. Hence, we can conclude that tRNA binding with neutral and protonated A-C pairs is almost isoenergetic and that protonation does not remove the high-selectivity states.

Instead, we predict that the existence of high-selectivity On states and low-selectivity Off states, in fact, provides a very efficient way of controlling the error frequency in translation that can be utilized both during initial selection and proofreading (Figure 4). At the proofreading stage, noncognate substrates will preferentially fall back into the A/T:Off state and dissociate precisely because the accommodated A/A:On state leading to peptide bond formation is higher in energy for noncognates, because of its stronger discrimination between correct and incorrect substrates. Cognate substrates, on the other hand, will spontaneously accommodate and undergo peptidyl transfer provided that their A/A:On state lies downhill (Figure 4). The fact that this is indeed the case is suggested by the extremely low rate of dissociation from the accommodated state of ∼10^{-4} s^{-1} measured for Phe-RNA^{Phe},[41] which is more than 10000 times slower than the rate of rejection for noncognate subtrates.[3] This would correspond to the cognate A/A:On state lying ∼6 kcal/mol below the noncognate A/T:Off state, and thus being 1−2 kcal/mol downhill from the cognate A/T:Off state, provided that the transition states for rejection are similar (Figure 4).

Quantitative Example of Fidelity in Translation. To substantiate the decoding principle discussed above, it is useful to give numerical illustrations of how the existence of both low-selectivity (Off) and high-selectivity (On) intermediate states can be used to drive rejection of noncognate substrates. A key feature of our model is that the rate constants for the elementary chemical steps need not differ, thus removing the requirement for codon-dependent long-range signaling between the decoding site and the (GTPase and peptidyl transferase) chemical reaction centers 75 Å away. This is shown in Table 1, where the calculated energetics for the high-selectivity A/T:On state is merged with the kinetic data of Rodnina and co-workers for first position UUC and CUC codon reading by tRNA^{Phe}.[8] Here, the cognate GTPase and GTP hydrolysis rates[8] are assumed to be the same (120 s^{-1}), and the cognate A/T:On state is placed 1 kcal/mol [=RT ln(k_{-2}/k_2)] below the A/T:Off state. The experimental selectivity in the A/T:Off state is RT ln(100/0.12) = 4 kcal/mol. The value of the noncognate k_{-2} comes from our calculated selectivity in the A/T:On state (Figure 2) of ∼8 kcal/mol; i.e., RT ln$(k_{-2}/k_2)_{noncog}$ − RT ln$(k_{-2}/k_2)_{cog}$ + 4 kcal/mol = 8 kcal/mol. For this three-step scheme, we have

$$k_{cat} = \frac{k_2 k_3}{k_2 + k_{-2} + k_3} \quad (1)$$

and

$$\frac{k_{cat}}{K_M} = \frac{k_1 k_2 k_3}{k_2 k_3 + k_{-1} k_{-2} + k_{-1} k_3} \quad (2)$$

which results in k_{cat}/K_M values of 140 and 1.3 μM^{-1} s^{-1} for cognate and noncognate codons, respectively. The absolute magnitude of these is of course dependent on the effective association rate constant[8] k_1, but their ratio is independent. This ratio is the accuracy factor or fidelity of initial selection, which the model predicts to be ∼100 under these conditions, in good agreement with the experiments.[8] The difference in binding free energy (corresponding to a factor of ∼1000) is not fully used in discrimination because the rate-limiting steps are different for cognate (codon recognition) and noncognate (GTP hydrolysis) substrates, as pointed out earlier.[10] Note, however, that the model does not exclude the possibility that the free energy barrier for the GTPase activation step is higher for noncognate substrates.

The accuracy is, however, critically dependent on the actual value of the cognate dissociation constant k_{-1}, so that it increases linearly toward its maximal value as k_{-1} increased, as long as the k^{nc}_{-1}/k^{c}_{-1} ratio is constant.[5] It can thus be noted that the accuracy is determined both by the difference in the dissociation

dx.doi.org/10.1021/bi5000355 | Biochemistry 2014, 53, 1714−1722

Table 2. Numerical Example of Accuracy for tRNA^{Phe} in Proofreading[a]

rate constant (s^{-1})	cognate (UUC)	noncognate (CUC)	$\Delta G_{cognate}$ (kcal/mol)	$\Delta G_{noncognate}$ (kcal/mol)	
k_{rej}	0.01	7	20.6	20.6	$\ddagger_1$
k_2 (A/T:Off → A/T:On)	120	120	0	4.1	A/T:Off
k_{-2} (A/T:On → A/T:Off)	20	15000	14.8	18.9	$\ddagger_2$
k_{pep}	50	50	−1.1	7.0	A/T:On
k_{cat}	43	0.4	14.3	22.4	$\ddagger_3$
$f = \frac{(k_2 + k_{rej})k_{pep}}{k_2k_{pep} + k_{-2}k_{rej} + k_{pep}k_{rej}}$	1.0	0.06			

[a]Experimental rate constants are k_{rej} for noncognate[3] tRNA and k_{pep} for cognate,[3,11] where the latter is the typical value reported for accommodation and peptide bond formation. The value of k_{rej} for the cognate substrate from the A/T:Off state is determined by requiring that this state have the same experimental selectivity as in initial selection (Table 1). The apparent rate of rejection of cognate tRNA from the accommodated A/A:On will be significantly lower than k_{rej} as observed experimentally[41] because the A/A:On state is presumably further downhill from A/T:On. Columns 5 and 6 give the free energies of activation barriers (numbered 1−3 from the left in Figure 4) and intermediate states relative to the cognate A/T:Off state, respectively, as in Table 1, where the first entry is the barrier height for rejection. The last entry gives the factors, f, that determine the additional proofreading selection (eq 3). Note that the On ↔ Off activation barrier can be increased somewhat without any significant effect on the results.

free energy barriers (18.9 and 14.9 kcal/mol for cognate and noncognate tRNAs, respectively) and by the barriers for the rate-limiting forward steps. In the cognate case, the forward flow from the A/T:Off state is limited by GTPase activation (14.8 kcal/mol), while in the noncognate case, the GTP hydrolysis step is limiting with a total free energy barrier that includes the activation step. This barrier is thus 21.7 kcal/mol − 4.0 kcal/mol = 17.7 kcal/mol, yielding an apparent GTP hydrolysis rate of ∼1 s^{-1} (Table 1), in good agreement with the experiment.[8] It is thus apparent that part of the high selectivity in the A/T:On state is masked by the cognate and noncognate substrates having different rate-limiting steps. A recent kinetic analysis has suggested that this type of free energy landscape is also optimal for decoding.[42]

The same type of analysis, based on the diagram of Figure 4, can be applied to the proofreading stage that illustrates how the existence of high-selectivity On states again can partition the flow of cognate and noncognate tRNAs differently toward peptide bond formation and rejection, respectively (Table 2). The key quantity here is then the proofreading selection factor F, which in terms of rate constants is given by

$$F = \left[\frac{(k_2 + k_{rej})k_{pep}}{k_2k_{pep} + k_{-2}k_{rej} + k_{pep}k_{rej}}\right]_{cog} \Bigg/ \left[\frac{(k_2 + k_{rej})k_{pep}}{k_2k_{pep} + k_{-2}k_{rej} + k_{pep}k_{rej}}\right]_{noncog} \quad (3)$$

where the rejection rates, k_{rej}, and the rates of transition from A/T:On to A/T:Off, k_{-2}, are the only ones assumed to differ between cognate and noncognate substrates. A ∼20-fold lower level of accuracy is obtained for proofreading in this example because of the free energy barriers for rejection being 1−2 kcal/mol higher than those for dissociation in initial selection (Table 1).

DISCUSSION

These free energy simulations clearly demonstrate that tRNA binding energetics on the ribosome varies dramatically between different conformational states. In particular, the results show for the first time, quantitatively, how switching of the small ribosomal subunit between its Off and On states amplifies the selectivity of the system. Somewhat surprisingly, we find that the key role of the 16S rRNA switch involving A1492, A1493, and G530 is not actually to monitor Watson−Crick base pairing but to shield the codon−anticodon base pair from solvent, whereby selectivity against incorrect substrates increases. This is also in line with a recent proposal that the high repulsion energy for near-cognate tRNAs in the On state(s) is what drives their dissociation from the ribosome.[18] It thus appears that both cognate and (nonrejected) noncognate complexes must pass through the On states to proceed forward. This is, in fact, supported both by recent crystal structures of near-cognate complexes[18] and by single-molecule FRET data.[22] The amplifying power of the Off → On switch is then reflected by the ∼3 kcal/mol increased level of discrimination that is attained in the solvent-shielded On states. Likewise, it seems logical that noncognate rejection should occur via the Off states, because they correspond to an "unlocking" of the 30S subunit that would seem to be necessary for rapid tRNA rejection. Moreover, the energetics (Figure 4) predicts that stabilization of the A/T:On state for both cognate and noncognate substrates would lead to an increased error. This is likely to be the mechanism of the increased error frequency caused either by binding of paromomycin or by high Mg^{2+} concentration, both of which appear to thermodynamically drive the switch to the On state.[8,18,43]

The kinetic model emerging from the free energy diagram of Figure 4 is also attractive in that it essentially makes codon-dependent long-range signaling between the decoding site and either of the peptidyl transferase and GTPase sites unnecessary (both being ∼75 Å away). On the other hand, it does not exclude the possibility that the free energy barrier for the GTPase activation step is higher for noncognate substrates, as mentioned above. However, the key structural "signals" for the GTP hydrolysis and peptidyl transfer reactions would be that the system is in the A/T:On and A/A:On states, respectively, regardless of whether the substrate is cognate or noncognate. More precisely, the existence of thermodynamically hidden high-selectivity states is what gives different apparent cognate and noncognate rate constants for GTP hydrolysis and peptide bond formation. That is, the rate constants for the elementary chemical steps of GTP hydrolysis and peptidyl transfer need not differ between cognate and noncognate substrates, once the GTPase-activated and -accommodated On states have been reached (with different probabilities for different substrates). The reactivities of truncated substrates, such as puromycin and derivatives thereof, support this notion.[44,45] However, the corresponding apparent (compounded) rates would indeed differ for incorrect tRNAs

dx.doi.org/10.1021/bi5000355 | Biochemistry 2014, 53, 1714−1722

because they include the probability ($\ll$1) of reaching the productive A/T:On and A/A:On states for GTP hydrolysis and peptidyl transfer, respectively, from their lowest-energy A/T:Off state. The alternative would be that the rates of the elementary chemical steps actually differ for cognate and noncognate substrates, because of mispositioning of the substrate[46] in the reaction centers caused by codon–anticodon mismatches far away, but available crystal structures[18,47] do not seem to support this idea for the ribosome. The high-selectivity states are hidden in the sense that they are inaccessible to binding measurements for noncognate substrates but evidently exist[18] and are amenable to computational analysis.

■ ASSOCIATED CONTENT

Supporting Information

Tests of the sensitivity of the computer simulations to the initial structural models and to the MD force field used and evaluation of the energetics of mRNA mutations in the absence of tRNA and of the effects of switching conformations of the monitoring bases individually. This material is available free of charge via the Internet at http://pubs.acs.org.

■ AUTHOR INFORMATION

Corresponding Author

*E-mail: aqvist@xray.bmc.uu.se. Phone: +46 18 471 4109.

Funding

This work was supported by the Swedish Research Council (VR), the Knut and Alice Wallenberg Foundation, and the Swedish National Infrastructure for Computing (SNIC).

Notes

The authors declare no competing financial interest.

■ ACKNOWLEDGMENTS

We thank Prof. Måns Ehrenberg for useful discussions.

■ ABBREVIATIONS

EF-Tu, elongation factor Tu; MD, molecular dynamics; ms^{2}i^{6}A, 2-methylthio-N6-isopentenyladenosine.

■ REFERENCES

(1) Rodnina, M. V., and Wintermeyer, W. (2001) Fidelity of aminoacyl-tRNA selection on the ribosome: Kinetic and structural mechanisms. *Annu. Rev. Biochem. 70*, 415–430.

(2) Ehrenberg, M., and Kurland, C. G. (1984) Costs of accuracy determined by a maximal growth rate constraint. *Q. Rev. Biophys. 17*, 45–82.

(3) Wohlgemuth, I., Pohl, C., and Rodnina, M. V. (2010) Optimization of speed and accuracy of decoding in translation. *EMBO J. 29*, 3701–3709.

(4) Kramer, E. B., and Farabaugh, P. J. (2007) The frequency of translational misreading errors in *E. coli* is largely determined by tRNA competition. *RNA 13*, 87–96.

(5) Johansson, M., Zhang, J., and Ehrenberg, M. (2012) Genetic code translation displays a linear trade-off between efficiency and accuracy of tRNA selection. *Proc. Natl. Acad. Sci. U.S.A. 109*, 131–136.

(6) Johansson, M., Ieong, K. W., Trobro, S., Strazewski, P., Åqvist, J., Pavlov, M. Y., and Ehrenberg, M. (2011) pH-sensitivity of the ribosomal peptidyl transfer reaction dependent on the identity of the A-site aminoacyl-tRNA. *Proc. Natl. Acad. Sci. U.S.A. 108*, 79–84.

(7) Ogle, J. M., Murphy, F. V., Tarry, M. J., and Ramakrishnan, V. (2002) Selection of tRNA by the ribosome requires a transition from an open to a closed form. *Cell 111*, 721–732.

(8) Gromadski, K. B., Daviter, T., and Rodnina, M. V. (2006) A uniform response to mismatches in codon-anticodon complexes ensures ribosomal fidelity. *Mol. Cell 21*, 369–377.

(9) Almlöf, M., Andér, M., and Åqvist, J. (2007) Energetics of Codon-Anticodon Recognition on the Small Ribosomal Subunit. *Biochemistry 46*, 200–209.

(10) Gromadski, K. B., and Rodnina, M. V. (2004) Kinetic determinants of high-fidelity tRNA discrimination on the ribosome. *Mol. Cell 13*, 191–200.

(11) Johansson, M., Bouakaz, E., Lovmar, M., and Ehrenberg, M. (2008) The kinetics of ribosomal peptidyl transfer revisited. *Mol. Cell 30*, 589–598.

(12) Thompson, R. C., and Stone, P. J. (1977) Proofreading of the codon-anticodon interaction on ribosomes. *Proc. Natl. Acad. Sci. U.S.A. 74*, 198–202.

(13) Ruusala, T., Ehrenberg, M., and Kurland, C. G. (1982) Is there proofreading during polypeptide synthesis? *EMBO J. 1*, 741–745.

(14) Wimberly, B. T., Brodersen, D. E., Clemons, W. M., Jr., Morgan-Warren, R. J., Carter, A. P., Vonrhein, C., Hartsch, T., and Ramakrishnan, V. (2000) Structure of the 30S ribosomal subunit. *Nature 407*, 327–339.

(15) Voorhees, R. M., Schmeing, T. M., Kelley, A. C., and Ramakrishnan, V. (2010) The mechanism for activation of GTP hydrolysis on the ribosome. *Science 330*, 835–838.

(16) Voorhees, R. M., Weixlbaumer, A., Loakes, D., Kelley, A. C., and Ramakrishnan, V. (2009) Insights into substrate stabilization from snapshots of the peptidyl transferase center of the intact 70S ribosome. *Nat. Struct. Mol. Biol. 16*, 528–533.

(17) Jenner, L. B., Demeshkina, N., Yusupova, G., and Yusupov, M. (2010) Structural aspects of messenger RNA reading frame maintenance by the ribosome. *Nat. Struct. Mol. Biol. 17*, 555–560.

(18) Demeshkina, N., Jenner, L., Westhof, E., Yusupov, M., and Yusupova, G. (2012) A new understanding of the decoding principle on the ribosome. *Nature 21*, 256–259.

(19) Schuette, J. C., Murphy, F. V., IV, Kelley, A. C., Weir, J. R., Giesebrecht, J., Connell, S. R., Loerke, J., Mielke, T., Zhang, W., Penczek, P. A., Ramakrishnan, V., and Spahn, C. M. (2009) GTPase activation of elongation factor EF-Tu by the ribosome during decoding. *EMBO J. 28*, 755–765.

(20) Valle, M., Zavialov, A., Sengupta, J., Rawat, U., Ehrenberg, M., and Frank, J. (2003) Locking and unlocking of ribosomal motions. *Cell 114*, 123–134.

(21) Blanchard, S. C., Gonzalez, R. L., Kim, H. D., Chu, S., and Puglisi, J. D. (2004) tRNA selection and kinetic proofreading in translation. *Nat. Struct. Mol. Biol. 11*, 1008–1014.

(22) Geggier, P., Dave, R., Feldman, M. B., Terry, D. S., Altman, R. B., Munro, J. B., and Blanchard, S. C. (2010) Conformational sampling of aminoacyl-tRNA during selection on the bacterial ribosome. *J. Mol. Biol. 399*, 576–595.

(23) Sund, J., Andér, M., and Åqvist, J. (2010) Principles of stop-codon reading on the ribosome. *Nature 465*, 947–950.

(24) Marelius, J., Kolmodin, K., Feierberg, I., and Åqvist, J. (1998) Q: A molecular dynamics program for free energy calculations and empirical valence bond simulations in biomolecular systems. *J. Mol. Graphics Modell. 16*, 213–225.

(25) Yusupova, G., Jenner, L., Rees, B., Moras, D., and Yusupov, M. (2006) Structural basis for messenger RNA movement on the ribosome. *Nature 444*, 391–394.

(26) Zhang, W., Dunkle, J. A., and Cate, J. H. D. (2009) Structures of the ribosome in intermediate states of ratcheting. *Science 325*, 1014–1017.

(27) King, G., and Warshel, A. (1989) A surface constrained all-atom solvent model for effective simulations of polar solutions. *J. Chem. Phys. 91*, 3647–3661.

(28) Lee, F. S., and Warshel, A. (1992) A local reaction field method for fast evaluation of long-range electrostatic interactions in molecular simulations. *J. Chem. Phys. 97*, 3100–3107.

(29) MacKerell, A. D., Jr., Bashford, D., Bellott, M., Dunbrack, R. L., Jr., Evanseck, J. D., Field, M. J., Fischer, S., Gao, J., Guo, H., Ha, S., Joseph-

McCarthy, D., Kuchnir, L., Kuczera, K., Lau, F. T. K., Mattos, C., Michnick, S., Ngo, T., Nguyen, D. T., Prodhom, B., Reiher, W. E., III, Roux, B., Schlenkrich, M., Smith, J. C., Stote, R., Straub, J., Watanabe, M., Wiorkiewicz-Kuczera, J., Yin, D., and Karplus, M. (1998) All-atom empirical potential for molecular modeling and dynamics studies of proteins. *J. Phys. Chem. B 102*, 3586−3616.
(30) MacKerell, A. D., Wiorkiewiczkuczera, J., and Karplus, M. (1995) An all-atom empirical energy function for the simulation of nucleic-acids. *J. Am. Chem. Soc. 117*, 11946−11975.
(31) Pérez, A., Marchán, I., Svozil, D., Sponer, J., Cheatham, T. E., III, Laughton, C. A., and Orozco, M. (2007) Refinement of the AMBER force field for nucleic acids, improving the description of α/γ conformers. *Biophys. J. 92*, 3817−3829.
(32) Hornak, V., Abel, R., Okur, A., Strockbine, B., Roitberg, A., and Simmerling, C. (2006) Comparison of multiple Amber force fields and development of improved protein backbone parameters. *Proteins 65*, 712−725.
(33) Ogle, J. M., Brodersen, D. E., Clemons, W. M., Jr., Tarry, M. J., Carter, A. P., and Ramakrishnan, V. (2001) Recognition of cognate transfer RNA by the 30S ribosomal subunit. *Science 292*, 897−902.
(34) Selmer, M., Dunham, C. M., Murphy, F. V., IV, Weixlbaumer, A., Petry, S., Kelley, A. C., Weir, J. R., and Ramakrishnan, V. (2006) Structure of the 70S ribosome complexed with mRNA and tRNA. *Science 313*, 1935−1342.
(35) Åqvist, J. (1994) Comment on the transferability of ion models. *J. Phys. Chem. 98*, 8253−8255.
(36) Fourmy, D., Yoshizawa, S., and Puglisi, J. D. (1998) Paromomycin binding induces a local conformational change in the A-site of 16 S rRNA. *J. Mol. Biol. 277*, 333−345.
(37) Daviter, T., Wieden, H. J., and Rodnina, M. V. (2003) Essential role of histidine 84 in elongation factor Tu for the chemical step of GTP hydrolysis on the ribosome. *J. Mol. Biol. 332*, 689−699.
(38) Wallin, G., Kamerlin, S. C. L., and Åqvist, J. (2013) Energetics of activation of GTP hydrolysis on the ribosome. *Nat. Commun. 4*, 1733.
(39) Paglieri, L., Corongiu, G., and Estrin, D. A. (1995) Solvent effects in density functional calculations of uracil and cytosine tautomerism. *Int. J. Quantum Chem. 56*, 615−625.
(40) Jang, S. B., Hung, L. W., Chi, Y. I., Holbrook, E. L., Carter, R. J., and Holbrook, S. R. (1998) Structure of an RNA internal loop consisting of tandem C-A^+ base pairs. *Biochemistry 37*, 11726−11731.
(41) Fahlman, R. P., Dale, T., and Uhlenbeck, O. C. (2004) Uniform binding of aminoacylated transfer RNAs to the ribosomal A and P sites. *Mol. Cell 16*, 799−805.
(42) Savir, Y., and Tlusty, T. (2013) The ribosome as an optimal decoder: A lesson in molecular recognition. *Cell 153*, 471−479.
(43) Pape, T., Wintermeyer, W., and Rodnina, M. V. (2000) Conformational switch in the decoding region of 16S rRNA during aminoacyl-tRNA selection on the ribosome. *Nat. Struct. Mol. Biol. 7*, 104−107.
(44) Katunin, V. I., Muth, G. W., Strobel, S. A., Wintermeyer, W., and Rodnina, M. V. (2002) Important contribution to catalysis of peptide bond formation by a single ionizing group within the ribosome. *Mol. Cell 10*, 339−346.
(45) Brunelle, J. L., Youngman, E. M., Sharma, D., and Green, R. (2006) The interaction between C75 of tRNA and the A loop of the ribosome stimulates peptidyl transferase activity. *RNA 12*, 33−39.
(46) Prasad, B. R., Kamerlin, S. C. L., Florian, J., and Warshel, A. (2012) Prechemistry barriers and checkpoints do not contribute to fidelity and catalysis as long as they are not rate limiting. *Theor. Chem. Acc. 131*, 1288.
(47) Schmeing, T. M., Vorhees, R. M., Kelley, A. C., and Ramakrishnan, V. (2011) How mutations in tRNA distant form the anticodon affect the fidelity of decoding. *Nat. Struct. Mol. Biol. 18*, 432−436.